

## SPECTRUM AND YIELD TO DOSE CONVERSION COEFFICIENTS FOR BETA SKIN DOSES LINKED TO THE Q SYSTEM

Thomas Frosio,<sup>1</sup> Philippe Bertreix,<sup>1</sup> Ulli Köster,<sup>2</sup> Christian Theis,<sup>1</sup> and Matteo Magistris<sup>1</sup>

**Abstract**—Monte Carlo simulations are a state-of-the-art method to calculate dose coefficients and could be used with the Q system for radioactive material packaging. These simulations often take a long time to converge with sufficient precision. Furthermore, if multiple sources have to be taken into account, many weeks of calculations may be needed. In order to reduce the calculation time, this paper proposes a new method based on a transfer function to instantly compute  $Q$  values associated with beta skin doses. The method developed in this paper can be applied to compute beta skin dose and easily could be extended to other particles and different depths in organs with various kinds of shielding configurations between source and target.

Health Phys. 116(5):607–618; 2019

**Key words:** contamination; dose, skin; radiation protection; safety standards

---

### INTRODUCTION

CALCULATIONS of beta skin dose are useful for different purposes such as radiation protection (transport and handling of radioactive material) or medical applications. The dose originating from beta emissions is often difficult to assess as beta particles have a finite range and keep changing their lineal energy transfer during their slowdown in matter. For photons, the interpolation of the dose depending on the thickness of shielding can be performed by considering the attenuation following an exponential function. For the beta dose, this is less straightforward.

Beta skin doses from different sources at different distances can be found in the literature. Some have been

calculated in air at 10 cm from the source (Petoussi et al. 1993) or can be found in vacuum at 10 cm for different depths of skin (Veinot and Hertel 2010).

The Q system is a methodology whereby a series of exposure scenarios is considered, each of which may result in the exposure to radiation (external or internal) of persons in the vicinity of a Type A package involved in a transportation accident.

The dosimetric pathways considered lead to five limits:  $Q_A$  for the external dose due to photons,  $Q_B$  for the external dose to the skin due to beta emitters,  $Q_C$  for the internal dose via inhalation,  $Q_D$  for the dose due to skin contamination, and  $Q_E$  for the dose by submersion.  $A_1$  is defined as the minimum value of  $Q_A$  and  $Q_B$ , and  $A_2$  is defined as the minimum value of all the  $Q_x$  quantities.

Values of these different  $Q_x$  quantities can be found in the International Atomic Energy Agency (IAEA) safety regulation SSG-26 (IAEA 2012), but not all radionuclides are presented in this document.

In this paper, the purpose is to introduce a transfer function that can be directly used with source nuclear data to compute the desired value of beta skin dose in accordance with the Q system. To validate the method based on transfer functions, some radionuclides will also be calculated with the FLUKA particle transport code (Ferrari et al. 2005; Battistoni et al. 2015) as a predefined radiation source with the HI-PROP option. This kind of calculation will be referred to as the source method in the next sections.

### MATERIALS AND METHODS

Monte Carlo simulations are nowadays a state-of-the-art method in various radiation transport problems. However, their use sometimes incurs long calculation times to achieve results with sufficient statistical significance. As an alternative, a transfer function build with FLUKA v. 2011.2c.6 Monte Carlo calculations is introduced in order to calculate  $Q_B$  and  $Q_D$  for a given radionuclide without further Monte Carlo simulations.

<sup>1</sup>Radiation Protection Group, European Organization for Nuclear Research, Geneva, Switzerland; <sup>2</sup>Institut Laue Langevin, Grenoble, France.

The authors declare no conflicts of interest.

For correspondence contact Thomas Frosio, Radiation Protection Group, European Organization for Nuclear Research, 1211, Geneva 23, Switzerland, or email at [thomas.frosio@cern.ch](mailto:thomas.frosio@cern.ch) or [thomas.frosio@gmail.com](mailto:thomas.frosio@gmail.com).

(Manuscript accepted 29 August 2018)

Supplemental digital content is available in the HTML and PDF versions of this article on the Journal's website [www.health-physics.com](http://www.health-physics.com).

0017-9078/19/0

Copyright © 2019 Health Physics Society

DOI: 10.1097/HP.0000000000000986

[www.health-physics.com](http://www.health-physics.com)

To avoid long calculation times, transfer functions will be produced with FLUKA to enable the calculation of  $Q_B$  and  $Q_D$  for a given radionuclide without any other simulation.

In the following, decay data are taken from the literature (ICRP 2008).

### Methods for $Q_A$ , $Q_C$ , $Q_E$ , and $Q_F$ calculation

**$Q_A$  coefficient.** The  $Q_A(r)$  coefficient is defined, for a given radionuclide  $r$ , as the external dose due to photons at a distance of 1 m from the source. It is calculated as follows:

$$Q_A(r) = \frac{10^{-13}}{e_{pt}(r)} \text{ (TBq)}, \quad (1)$$

where  $e_{pt}(r)$  is defined as the equivalent dose rate for 1 Bq due to x rays and gamma radiation at 1 m from the radiation source in air. The values of  $e_{pt}(r)$  are calculated using the following formula:

$$e_{pt}(r) = \frac{A}{4\pi d^2} C \sum_{i=1}^n D_i Y_i E_i \left( \frac{\mu_{en}}{\rho} \right)_i e^{-\mu_i d} B(E_{i,d}), \quad (2)$$

where

$A$  = activity of the source in Bq;

$d$  = distance between the source and the calculation point in cm;

$n$  = number of distinct photon emissions;

$D_i$  = conversion coefficient for kerma to effective dose in air in  $\text{Sv Gy}^{-1}$ ;

$Y_i$  = yield of the photon emission at energy  $E_i$  in MeV;

$\left( \frac{\mu_{en}}{\rho} \right)_i$  = energy absorption coefficient for photon  $i$  in  $\text{cm}^2 \text{ g}^{-1}$ ;

$\mu_i$  = linear attenuation coefficient in air for photon  $i$  in  $\text{cm}^{-1}$ ;

$B(E_{i,d})$  = build-up factor for energy  $E_i$  at a distance  $d$  from the radiation source; and

$C$  = dimensional constant ( $5.768 \times 10^{-7} \text{ Gy h}^{-1} \text{ g s MeV}^{-1}$ ).

To calculate  $e_{pt}(r)$ , we use the most recently published International Commission on Radiological Protection (ICRP) values of the effective dose to kerma conversion coefficient in air (ICRP 2010).

In order to determine  $D_i$  values for any energy, a linear interpolation was performed for energies ranging from 10 keV to 20 MeV. The values of the energy absorption coefficients and attenuation coefficients are directly extracted from the XMuDat software (Nowotny 1998).

**$Q_C$  coefficient.** The  $Q_C(r)$  coefficient is defined, for a given radionuclide, as the inhalation dose. It is calculated as follows:

$$Q_C(r) = \frac{5 \times 10^{-8}}{e_{inh}(r)} \text{ (TBq)}, \quad (3)$$

where  $e_{inh}(r)$  is defined as the effective dose coefficient for inhalation of a given radionuclide in  $\text{Sv Bq}^{-1}$ . The values of  $e_{inh}(r)$  are from different publications (ICRP 2012; JAERI 2002; IAEA 2012). From these three publications, the most conservative  $e_{inh}(r)$  value is retained when the progeny are taken into account:

- $e_{inh}(r)$  (IAEA 2012) take into account progeny with half-lives less than the half-life of the parent and less than 10 d; and
- $e_{inh}(r)$  from other sources (ICRP 2012; JAERI 2002) take into account all the progeny, which leads to more conservative values.

Note that  $e_{inh}(r)$  coefficients depend on the radionuclide's chemical form and the particle size. For this work, the most penalizing chemical form was used. The activity median aerodynamic diameter (AMAD) of 1  $\mu\text{m}$  was used, even if an AMAD of 5  $\mu\text{m}$  is more restrictive (IAEA 2012).

**$Q_E$  coefficient.** The  $Q_E(r)$  coefficient is defined as the dose due to immersion in a radioactive cloud. This coefficient is only valid for gaseous radioelements. It then replaces the  $Q_D(r)$  coefficient. As this document does not focus on such forms, this coefficient will not be discussed further in this model.

**$Q_F$  coefficient.** In the Q system, a radionuclide is defined as an alpha emitter if in 0.1% of its decays, an alpha particle is emitted, or if the progeny radionuclide is an alpha emitter. In this case, in general, the calculation of  $Q_A(r)$  or  $Q_B(r)$  for special form radionuclides is irrelevant, given the low beta and gamma emissions they produce.

Nevertheless, the doses due to inhalation of this type of radionuclide can be very important. The factor  $Q_F(r)$  is defined as:

$$Q_F(r) = 10^4 Q_C(r). \quad (4)$$

If it is more restrictive, this factor will replace  $Q_A(r)$  only for special form radionuclides.

### Computation of the transfer function and method to produce $Q_B$ and $Q_D$

The  $Q_B$  quantity describes the skin dose due to electron emissions from the source. It represents the beta dose to the skin  $H_p(0.07)$  at 100 cm from the source in air for a damaged package (IAEA 2012; Benassai and Bologna 1994; Eckerman and Ryman 1993).

The  $Q_D(r)$  coefficient for a radionuclide  $r$  describes the beta dose to the skin of a contaminated

person. Different hypotheses are assumed. Considering an accident during transport, it is assumed that 1% of the package has been spread uniformly over a 1 m<sup>2</sup> area (IAEA 2012).

Transfer functions for both electrons and positrons have been produced with FLUKA at different energies. An isotropic beam of electrons/positrons is placed in the center of the geometry (Fig. 1), and each calculation is performed with a different energy.

For this study, FLUKA v. 2011.2c.6 has been used with the PRECISION default setting. The energy threshold for electron production has been set to 350 keV for  $Q_B$  as the maximum range of 350 keV electrons in air is below 1 m, and 50 keV for  $Q_D$  as the maximum range of 50 keV electrons in skin is below 50  $\mu\text{m}$  (according to the continuous slowing down approximation [CSDA] range from the National Institute of Standards and Technology [NIST]), to reduce the simulation time. Photons are discarded to avoid the processes leading to secondary electron production from the environment by photoelectric effect, Compton effect, or pair production. Isotropic beams of electrons and positrons are generated with different kinetic energies. For  $Q_B$ , energies range from 0.35 to 12 MeV and for  $Q_D$ , from 0.05 to 12 MeV. These values have been selected for two main reasons:

- The upper bound corresponds to the maximum electron/positron energy which can be emitted by a radionuclide. The maximum energy for electrons from  $^{16}\text{N}$  is 10.42 MeV; and
- The lower bound corresponds to the minimum of energy at which the scoring volume experiences energy deposition.

### Methods for $Q_B$ calculation

It is assumed that a residual shield is retained and defined depending on the maximal energy of the electrons emitted by the source (IAEA 2012). This shielding factor

(SF) is applied as a residual dose-reduction factor and divides the calculated dose. A conservative SF of 3 for beta energies greater than 2 MeV is assumed (IAEA 2012); for positron emitters, annihilation photons are integrated into the  $Q_A$  coefficient.

In this work, the calculated SF has been applied with the following equation at all energies for more accuracy:

$$SF = e^{\mu d}, \quad (5)$$

where  $d$  is an absorber of approximately 150 mg cm<sup>-2</sup> thickness (IAEA 2012) and  $\mu = 0.017 \times E_{\beta, \text{max}}^{-1.14}$  is the apparent absorption coefficient in cm<sup>2</sup> mg<sup>-1</sup>.

For radionuclides that emit only monoenergetic electrons, there is no precise information about the shielding factor to use (IAEA 2012). In this case, the conservative factor of 3 has been used, without taking into account the maximum energy of the electrons.

For a radionuclide  $r$ ,  $Q_B$  is calculated as follows in TBq:

$$Q_B(r) = \frac{10^{-12}}{e_{\beta}(r)} \text{ (TBq)}, \quad (6)$$

where  $e_{\beta}(r)$  is the equivalent skin dose rate from a point source with electron emissions at 100 cm in air in Sv h<sup>-1</sup> Bq<sup>-1</sup>.

The model is constructed as a point source of different kinetic energies of electrons and positrons surrounded by a sphere of skin, as seen in Fig. 1. The sphere of skin has been defined with the goal of being everywhere at a distance of 1 m from the source.

The average energy deposited by electrons is recorded at the position of interest 0.07 mm below the skin surface. For that, a scoring volume is defined with an inner radius of 100.005 cm and an outer radius of 100.009 cm. The phantom skin is modeled as follows: 10.1% hydrogen, 11.1% carbon, 2.6% nitrogen, and 76% oxygen with a density of 1 g cm<sup>-3</sup> (ICRU 1993).

The transfer function depends on the particle energy, and this dependence is taken into account as follows:

$$e_{\beta}(r) = \frac{C_1}{SF} [\int_E H_{e^{\pm}, Q_B}(E) \xi(E, r) dE +$$

$$\sum_E H_{e^-, Q_B}(E) AE(E, r) + \sum_E H_{e^+, Q_B}(E) IC(E, r)], \quad (7)$$

where  $H_{e^{\pm}, Q_B}(E)$  is the transfer function expressed in GeV g<sup>-1</sup> beta<sup>-1</sup>, giving the skin dose in Sv beta<sup>-1</sup> ( $e^+$  or  $e^-$ ) emitted at energy  $E$  at 1 m from the skin and going through air.  $H_{e^{\pm}, Q_B}(E)$  is the result given by the FLUKA dose scores at energy  $E$ .

$\xi(E, r)$  is the beta spectrum of radionuclide  $r$  expressed as the number of betas emitted per nuclear transformation at energies between  $E$  and  $E+dE$ .

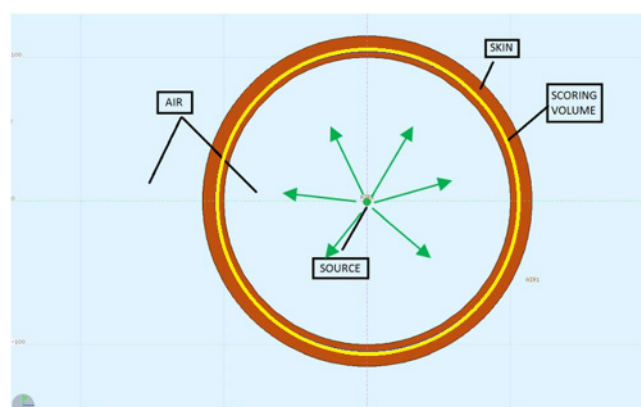


Fig. 1. Sphere of skin in air around the point source for the simulation of beta dose (scoring volume not to scale).

$IC(E, r)$  and  $AE(E, r)$  are the absolute yields of the radiation at energy  $E$  emitted by the processes of conversion electrons and Auger electrons, respectively.

Finally, SF is the shielding factor,  $C_1$  is a conversion factor to express  $J(r)$  in Gy, such as  $C_1 = 1.60218 \times 10^{-7} \times 3,600 \text{ J kg}^{-1} \text{ GeV}^{-1} \text{ g s h}^{-1}$ .

In the following, the  $C_1$  coefficient has been integrated into the transfer function. As a consequence, the transfer function can be directly multiplied by a binned beta spectrum as well as monoenergetic electrons to get a result with the adequate unit.  $\hat{H}_{e^\pm, Q_B}$  is the transfer function expressed in  $\text{Sv beta}^{-1}$ :

$$\hat{H}_{e^\pm, Q_B} = C_1 H_{e^\pm, Q_B}. \quad (8)$$

For this calculation, the transfer function  $\hat{H}_{e^\pm, Q_B}(E)$  is interpolated by constructing a rational fraction based on a nonlinear least-squares algorithm within the energy bins, and the integral is calculated by trapezoidal numerical approximations.

Fig. 2 shows particle equilibrium for a simulation of electron beams at different energies. It is observed that at 0.1 MeV, no electrons reach the skin. When the energy increases, electrons penetrate deeper into the skin.

Fig. 3 shows the transfer function for electrons and positrons  $\hat{H}_{e^\pm, Q_B}(E)$  per energy  $E$  in MeV, and Table 1 gives the corresponding values. The fit is performed as detailed above. A maximum is reached at 0.512 MeV with a value of  $2.2139 \times 10^{-11} \text{ Sv beta}^{-1}$  for positrons and at 0.516 MeV with  $2.2256 \times 10^{-11} \text{ Sv beta}^{-1}$  for electrons. The dose per energy rapidly increases to this maximum and then slowly decreases after to stagnate around  $8.6 \times 10^{-12} \text{ Sv beta}^{-1}$ . As photons have been discarded,

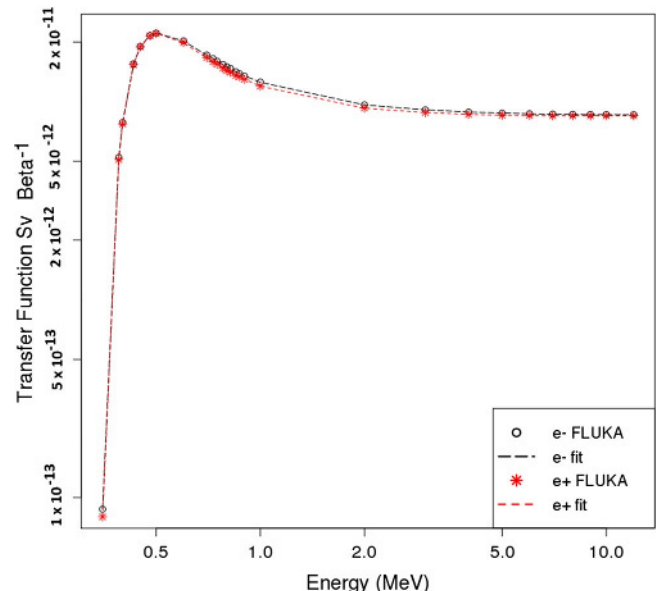


**Fig. 3.** Transfer function  $\hat{H}_{e^\pm, Q_B}(E)$  in  $\text{Sv beta}^{-1}$  for electrons and positrons.

and therefore annihilation photons do not create secondary electrons in the environment, greater importance of dose from positrons at low energy has not been observed as in other publications (Behrens 2017). Photons have been discarded to avoid taking them into account in the  $Q_B$  coefficient (IAEA 2012).

Fig. 4 uses the example of  $^{60}\text{Co}$  to represent all the different steps and intermediate results in getting the final dose. The black curve (number 1) represents the beta spectrum of the  $^{60}\text{Co}$  decay, and the red curve (number 2) represents the interpolated transfer function for electrons,

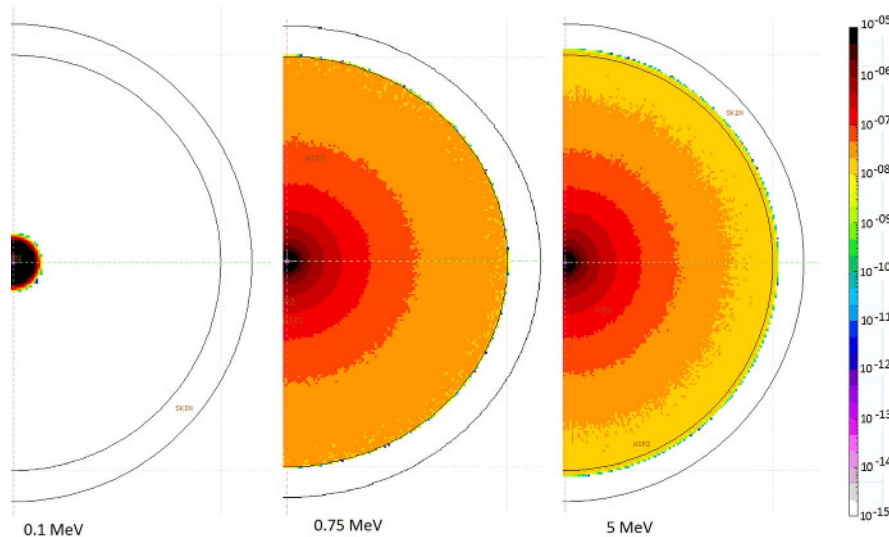


**Fig. 2.** Particle equilibrium in the geometry for sources of 0.1, 0.75, and 5 MeV electrons, respectively ( $\text{GeV g}^{-1} \text{ beta}^{-1}$ ).

depending on the energy. The blue curve (number 3) is the product of these two functions. A great part of the spectrum will be without interest for the dose calculation as, below 0.34 MeV, betas do not reach the scoring volume. Finally, the blue curve is integrated by the trapezoidal rule giving the green curve (number 4), which represents the surface under the blue curve. Then, the dose is the result of the blue curve integral, i.e., the last value reached by the green curve. The part of  $e_B(r)$  coming from the beta spectrum can be read directly from the green curve. It is the result of the integration over the entire energy range, and in the present example it has a value of around  $3.3 \times 10^{-15}$  Sv Bq<sup>-1</sup> h<sup>-1</sup>. The dose coming from monoenergetic electrons, such as conversion and Auger electrons, is added to this value using a

**Table 1.** Values of transfer function  $\hat{H}_{e^\pm, Q_B}(E)$  in Sv beta<sup>-1</sup> for electrons and positrons.

Energy of beta MeV	$\hat{H}_{e^\pm, Q_B}$		Uncertainty of transfer function	
	Transfer function for positron Sv beta <sup>-1</sup>	%	Transfer function for electron Sv beta <sup>-1</sup>	%
0.35	$7.99 \times 10^{-14}$	0.18%	$8.74 \times 10^{-14}$	0.23%
0.39	$5.10 \times 10^{-12}$	0.03%	$5.23 \times 10^{-12}$	0.03%
0.4	$7.73 \times 10^{-12}$	0.02%	$7.86 \times 10^{-12}$	0.02%
0.43	$1.54 \times 10^{-11}$	0.02%	$1.55 \times 10^{-11}$	0.02%
0.45	$1.89 \times 10^{-11}$	0.01%	$1.90 \times 10^{-11}$	0.03%
0.48	$2.15 \times 10^{-11}$	0.01%	$2.16 \times 10^{-11}$	0.01%
0.5	$2.21 \times 10^{-11}$	0.02%	$2.22 \times 10^{-11}$	0.02%
0.512	$2.21 \times 10^{-11}$	0.01%	—	—
0.516	—	—	$2.23 \times 10^{-11}$	0.01%
0.6	$1.99 \times 10^{-11}$	0.02%	$2.03 \times 10^{-11}$	0.02%
0.7	$1.67 \times 10^{-11}$	0.01%	$1.72 \times 10^{-11}$	0.02%
0.73	$1.59 \times 10^{-11}$	0.02%	$1.65 \times 10^{-11}$	0.02%
0.75	$1.55 \times 10^{-11}$	0.03%	$1.60 \times 10^{-11}$	0.02%
0.78	$1.48 \times 10^{-11}$	0.02%	$1.54 \times 10^{-11}$	0.02%
0.8	$1.44 \times 10^{-11}$	0.02%	$1.50 \times 10^{-11}$	0.02%
0.82	$1.41 \times 10^{-11}$	0.01%	$1.47 \times 10^{-11}$	0.01%
0.85	$1.36 \times 10^{-11}$	0.01%	$1.42 \times 10^{-11}$	0.03%
0.87	$1.34 \times 10^{-11}$	0.03%	$1.39 \times 10^{-11}$	0.03%
0.9	$1.30 \times 10^{-11}$	0.03%	$1.35 \times 10^{-11}$	0.03%
1	$1.20 \times 10^{-11}$	0.03%	$1.26 \times 10^{-11}$	0.01%
2	$9.30 \times 10^{-12}$	0.03%	$9.66 \times 10^{-12}$	0.01%
3	$8.82 \times 10^{-12}$	0.03%	$9.11 \times 10^{-12}$	0.02%
4	$8.63 \times 10^{-12}$	0.01%	$8.87 \times 10^{-12}$	0.02%
5	$8.55 \times 10^{-12}$	0.03%	$8.76 \times 10^{-12}$	0.03%
6	$8.53 \times 10^{-12}$	0.01%	$8.70 \times 10^{-12}$	0.03%
7	$8.50 \times 10^{-12}$	0.01%	$8.67 \times 10^{-12}$	0.01%
8	$8.50 \times 10^{-12}$	0.01%	$8.65 \times 10^{-12}$	0.00%
9	$8.50 \times 10^{-12}$	0.02%	$8.63 \times 10^{-12}$	0.01%
10	$8.50 \times 10^{-12}$	0.02%	$8.62 \times 10^{-12}$	0.05%
12	$8.50 \times 10^{-12}$	0.01%	$8.61 \times 10^{-12}$	0.02%

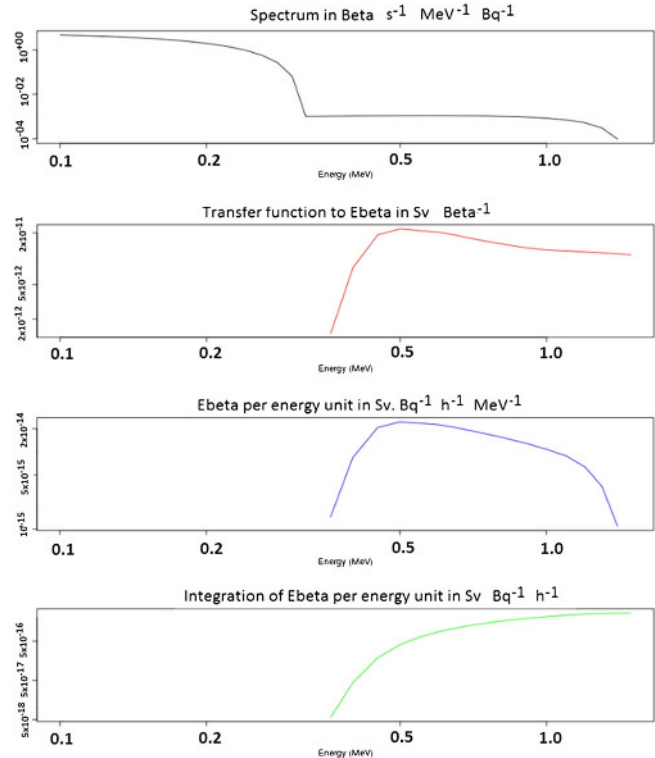


**Fig. 4.** Steps leading to the calculation of  $e_B(r)$ .

conservative shielding factor computed with the maximum energy of the beta spectrum of the radionuclide.

### Methods for $Q_D$ calculation

The  $Q_D(r)$  coefficient is defined as:

$$Q_D(r) = \frac{2.8 \times 10^{-2}}{h_{\text{skin}}(r)} (\text{TBq}), \quad (9)$$

where  $h_{\text{skin}}(r)$  represents the equivalent beta skin dose rate per disintegration per unit area of the skin in  $\text{Sv s}^{-1} \text{TBq}^{-1} \text{m}^2$ .

The model is constructed on a  $10 \times 10 \times 10 \text{ cm}^3$  skin slab as shown in Fig. 5.

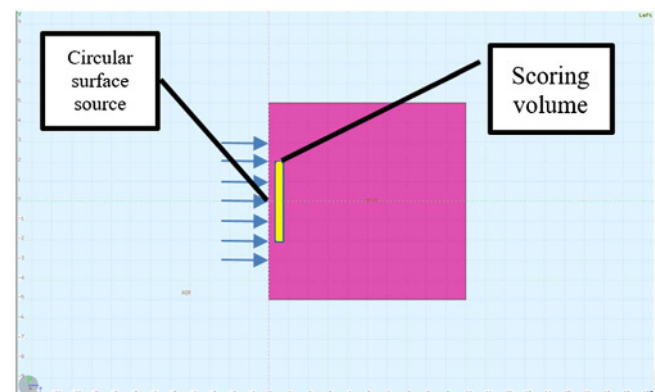


**Fig. 5.** Slab of skin in air in contact with the circular source of beta dose (scoring volume not to scale). The source is isotropically distributed.

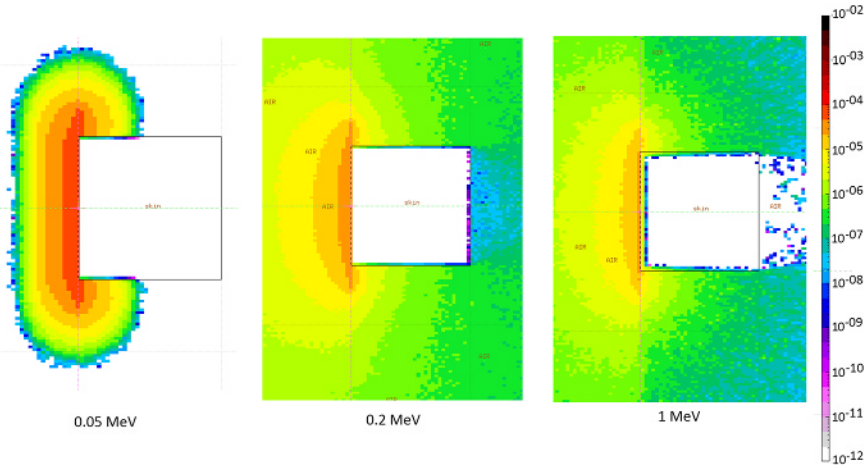


Fig. 6. Dose distribution for sources of electrons of different energies ( $\text{GeV g}^{-1} \text{beta}^{-1}$ ).

For the model presented in this paper, a circular-shaped source of electrons or positrons, respectively, is in contact with the skin. Fig. 6 shows the electron dose for different energies of primary radiation. Electrons with low energies, such as 0.05 MeV, are not transported far from the source, contrary to more energetic particles, e.g., 0.2 or 1 MeV. The surface source is isotropically distributed to take into account the angular distribution of particles in the problem, and the radius of the source is assumed to be 7 cm.

Scoring is performed in a cylinder with a radius of 0.5642 cm to cover a surface of  $1 \text{ cm}^2$ . This cylinder is centered on  $x = 0, y = 0$ , and  $z = 0.007 \text{ cm}$  for the beta dose skin  $H_p(0.07)$  and has a height of 0.004 cm. The scoring volume is very small compared to the skin dimensions and source in order to get an infinity configuration for the problem geometry (Fig. 7).

$h_{\text{skin}}(r)$  is calculated as follows:

$$h_{\text{skin}}(r) = C_2 \left[ \int_E H_{e^\pm, Q_D}(E) \xi(E, r) dE + \right.$$

$$\left. \sum_E H_{e^\pm, Q_D}(E) AE(E, r) + \sum_E H_{e^\pm, Q_D}(E) IC(E, r) \right]. \quad (10)$$

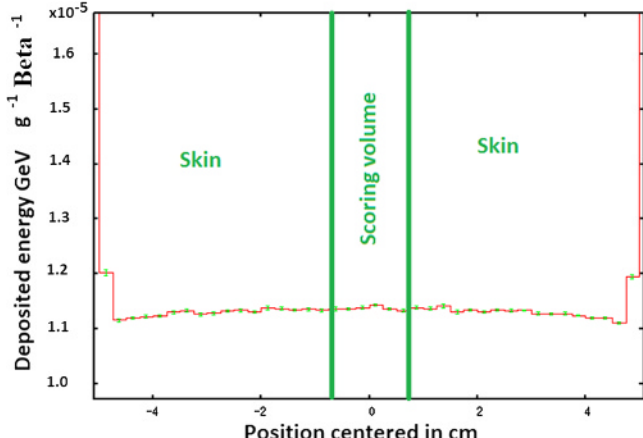


Fig. 7. Radial profile of energy deposition ( $\text{GeV g}^{-1} \text{beta}^{-1}$ ) in skin at 70  $\mu\text{m}$  depth.

As in the previous equation, symbols have the same meaning, except for  $H_{e^\pm, Q_D}(E)$ . This is the transfer function for electrons and positrons, expressed in  $\text{GeV g}^{-1} \text{beta}^{-1}$ , describing the skin dose due to surface contamination and  $C_2 = 1.60218 \times 10^{-7} \times \pi \times 7^2 \times 10^{-4} \text{ J kg}^{-1} \text{ GeV}^{-1} \text{ g TBq}^{-1} \text{ Bq m}^2 \text{ cm}^{-2} \text{ cm}^2$ . Values of  $H_{e^\pm, Q_D}$  are directly extracted from the FLUKA calculation code.

In the following, the  $C_2$  coefficient has been integrated into the transfer function. In this way, the transfer function can be directly multiplied by a binned beta spectrum, as well as data for monoenergetic electrons, to get a result with the adequate unit.  $\hat{H}_{e^\pm, Q_D}$  is the transfer function expressed as  $\text{Sv beta}^{-1} \text{ m}^2$ :

$$\hat{H}_{e^\pm, Q_D} = C_2 H_{e^\pm, Q_D}. \quad (11)$$

Fig. 8 depicts the transfer function  $\hat{H}_{e^\pm, Q_D}(E)$  for both electrons and positrons, depending on the energy. The fit is performed

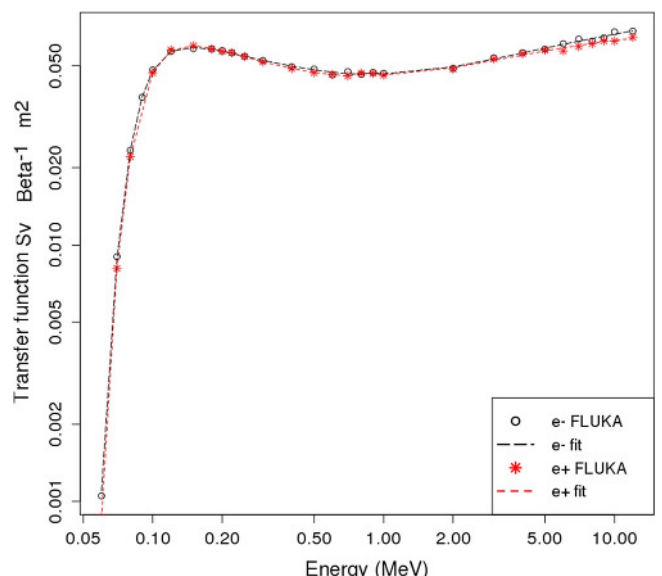


Fig. 8. Transfer function  $\hat{H}_{e^\pm, Q_D}(E)$  in  $\text{Sv beta}^{-1} \text{ m}^2$  for electrons and positrons.

**Table 2.** Values of transfer function  $\hat{H}_{e^\pm, Q_D}(E)$  in  $\text{Sv beta}^{-1} \text{m}^2$  for electrons and positrons.

$\hat{H}_{e^\pm, Q_D}$				
Energy of beta	Transfer function for positron	Uncertainty of transfer function for positron	Transfer function for electron	Uncertainty of transfer function for electron
MeV	$\text{Sv beta}^{-1} \text{m}^2$	%	$\text{Sv beta}^{-1} \text{m}^2$	%
0.06	$8.69 \times 10^{-04}$	2.69%	$1.05 \times 10^{-03}$	2.70%
0.07	$8.11 \times 10^{-03}$	1.22%	$9.01 \times 10^{-03}$	0.96%
0.08	$2.21 \times 10^{-02}$	0.72%	$2.34 \times 10^{-02}$	0.26%
0.09	$3.63 \times 10^{-03}$	0.68%	$3.77 \times 10^{-02}$	0.66%
0.1	$4.69 \times 10^{-02}$	0.53%	$4.81 \times 10^{-02}$	0.51%
0.140	—	—	$5.99 \times 10^{-02}$	0.64%
0.15	$5.98 \times 10^{-02}$	0.62%	$5.83 \times 10^{-02}$	0.63%
0.151	$6.01 \times 10^{-02}$	0.47%	—	—
0.18	$5.81 \times 10^{-02}$	0.64%	$5.81 \times 10^{-02}$	0.64%
0.2	$5.69 \times 10^{-02}$	0.65%	$5.72 \times 10^{-02}$	0.43%
0.22	$5.62 \times 10^{-02}$	0.44%	$5.61 \times 10^{-02}$	0.66%
0.25	$5.43 \times 10^{-02}$	0.45%	$5.43 \times 10^{-02}$	0.45%
0.3	$5.17 \times 10^{-02}$	0.72%	$5.24 \times 10^{-02}$	0.71%
0.4	$4.87 \times 10^{-02}$	1.27%	$4.95 \times 10^{-02}$	0.25%
0.5	$4.69 \times 10^{-02}$	1.05%	$4.85 \times 10^{-02}$	1.78%
0.6	$4.62 \times 10^{-02}$	0.80%	$4.60 \times 10^{-02}$	0.80%
0.7	$4.56 \times 10^{-02}$	1.08%	$4.74 \times 10^{-02}$	0.52%
0.8	$4.67 \times 10^{-02}$	1.32%	$4.62 \times 10^{-02}$	1.34%
0.9	$4.66 \times 10^{-02}$	0.53%	$4.70 \times 10^{-02}$	1.31%
1	$4.59 \times 10^{-02}$	2.68%	$4.67 \times 10^{-02}$	2.91%
2	$4.85 \times 10^{-02}$	1.27%	$4.88 \times 10^{-02}$	1.01%
3	$5.32 \times 10^{-02}$	0.70%	$5.36 \times 10^{-02}$	0.69%
4	$5.57 \times 10^{-02}$	1.77%	$5.61 \times 10^{-02}$	1.54%
5	$5.75 \times 10^{-02}$	1.72%	$5.80 \times 10^{-02}$	3.40%
6	$5.71 \times 10^{-02}$	2.80%	$6.09 \times 10^{-02}$	4.06%
7	$5.94 \times 10^{-02}$	0.83%	$6.35 \times 10^{-02}$	0.19%
8	$6.09 \times 10^{-02}$	1.22%	$6.23 \times 10^{-02}$	0.99%
9	$6.25 \times 10^{-02}$	0.59%	$6.42 \times 10^{-02}$	1.34%
10	$6.24 \times 10^{-02}$	1.97%	$6.78 \times 10^{-02}$	3.27%
12	$6.46 \times 10^{-02}$	1.90%	$6.82 \times 10^{-02}$	0.18%

as outlined previously. As seen in Table 2, the behavior of this function is a little different than the one of  $\hat{H}_{e^\pm, Q_B}(E)$ . The maximum dose is reached at 0.151 MeV with a value of  $6.009 \times 10^{-2} \text{ Sv beta}^{-1} \text{m}^2$  for positrons and at 0.140 MeV with a value of  $5.988 \times 10^{-2} \text{ Sv beta}^{-1} \text{m}^2$  for electrons. As for  $Q_B$ , the dose rapidly rises with the particle energy until reaching a maximum. From the maximum to

about 1 MeV, the dose decreases by about a quarter, then increases slowly by 40–50% to 12 MeV.

Fig. 9 shows the different quantities produced to compute  $h_{\text{skin}}(r)$  for  $^{60}\text{Co}$ . The beta spectrum is obviously the same as in Fig. 4. However, as the transfer function is different and gives doses for lower energies, the blue curve (number 3) corresponding to the product of these functions extends over a larger range compared to the blue curve built for the calculation of  $e_B(r)$ . Low-energy electrons are considered and have a bigger importance compared to  $e_B(r)$ . Moreover, as the emission probability is higher below 0.35 MeV, this part of the spectrum is responsible for the majority of the dose. This is why the green curve (number 4), which represents the surface under the blue curve, almost reaches its final value of  $h_{\text{skin}}(r) = 2.9 \times 10^{-2} \text{ Sv s}^{-1} \text{ TBq}^{-1} \text{ m}^2$  at 0.35 MeV. At this energy, the final value of the  $^{60}\text{Co}$  dose is almost reached because beta emissions with energies greater than 0.35 MeV are very low.

#### Analytical fit values for transfer functions

To allow the determination of transfer functions at other energies than those obtained with FLUKA, fit values are provided. These fit values are determined by the nonlinear least-squares Marquardt algorithm. They are modeled by a rational fraction as shown in eqn (12), where  $E$  represents the particle energy in MeV.

Coefficients for the eqn (12) rational fraction are listed in the Table 3.

## RESULTS

To compare the results of this method, the same radionuclides are calculated using FLUKA with a predefined radiation source (source method). Six radionuclides are used to compare with IAEA values:  $^7\text{Be}$ ,  $^{22}\text{Na}$ ,  $^{47}\text{Ca}$ ,  $^{58}\text{Co}$ ,  $^{60}\text{Co}$ , and  $^{137}\text{Cs}$ . Other radionuclides were used to validate the method of this paper. It is important to keep in mind that values from the Q system have to take into account the contribution of progeny nuclei whose half-lives are less than 10 d and are less than the parent radionuclide half-life. With the transfer function method, progeny have been taken into account by specifically calculating their  $e_B(r)$  or  $h_{\text{skin}}(r)$  and adding them to the parent nuclide value.

$$\left\{ \begin{array}{l} \log(\hat{H}_{e^\pm, Q_B}(E)) = \frac{a_0 + a_1 \log(E) + a_2 \log(E)^2 + a_3 \log(E)^3 + a_4 \log(E)^4 + a_5 \log(E)^5 + a_6 \log(E)^6}{b_0 + b_1 \log(E) + b_2 \log(E)^2 + b_3 \log(E)^3 + b_4 \log(E)^4 + b_5 \log(E)^5 + b_6 \log(E)^6} \\ \hat{H}_{e^\pm, Q_D}(E) = \frac{a_0 + a_1 E + a_2 E^2 + a_3 E^3 + a_4 E^4 + a_5 E^5 + a_6 E^6}{b_0 + b_1 E + b_2 E^2 + b_3 E^3 + b_4 E^4 + b_5 E^5 + b_6 E^6}. \end{array} \right. \quad (12)$$

**Table 3.** Coefficients for the rational fraction to fit transfer functions.

Energy range	$\hat{H}_{e^-, Q_B}$	$\hat{H}_{e^+, Q_B}$	$\hat{H}_{e^-, Q_D}$	$\hat{H}_{e^+, Q_D}$
	0.35 to 12 MeV	0.35 to 12 MeV	0.06 to 12 MeV	0.06 to 12 MeV
a0	$-2.874483 \times 10^{+01}$	$-2.922735 \times 10^{+01}$	$1.322601 \times 10^{-05}$	$1.796511 \times 10^{-04}$
a1	$-6.828859 \times 10^{+01}$	$-6.867395 \times 10^{+01}$	$-5.792672 \times 10^{-04}$	$-6.099799 \times 10^{-03}$
a2	$-1.162977 \times 10^{+01}$	$-1.179065 \times 10^{+01}$	$7.972477 \times 10^{-03}$	$4.975711 \times 10^{-02}$
a3	$-1.182617 \times 10^{+01}$	$-1.281269 \times 10^{+01}$	$-2.903328 \times 10^{-02}$	$4.800922 \times 10^{-02}$
a4	$-6.800606 \times 10^{+01}$	$-6.764020 \times 10^{+01}$	$-9.696325 \times 10^{-02}$	$-1.639161 \times 10^{-01}$
a5	$3.560588 \times 10^{+01}$	$3.482093 \times 10^{+01}$	$5.041241 \times 10^{-01}$	$-9.432847 \times 10^{-02}$
a6	$-4.259202 \times 10^{+01}$	$-4.212611 \times 10^{+01}$	$2.720633 \times 10^{-01}$	$1.767212 \times 10^{-01}$
b0	$2.636909 \times 10^{+00}$	$2.676373 \times 10^{+00}$	$3.138267 \times 10^{-04}$	$3.473286 \times 10^{-03}$
b1	$6.102521 \times 10^{+00}$	$6.121074 \times 10^{+00}$	$-8.098840 \times 10^{-03}$	$-5.691274 \times 10^{-02}$
b2	$1.006658 \times 10^{+00}$	$1.048664 \times 10^{+00}$	$5.134756 \times 10^{-02}$	$2.096265 \times 10^{-02}$
b3	$1.518168 \times 10^{+00}$	$1.625261 \times 10^{+00}$	$4.575033 \times 10^{-01}$	$5.085784 \times 10^{+00}$
b4	$5.210046 \times 10^{+00}$	$5.027323 \times 10^{+00}$	$-6.092683 \times 10^{+00}$	$-1.016277 \times 10^{+01}$
b5	$-2.388740 \times 10^{+00}$	$-2.126729 \times 10^{+00}$	$1.645164 \times 10^{+01}$	$2.884613 \times 10^{+00}$
b6	$3.582268 \times 10^{+00}$	$3.463855 \times 10^{+00}$	$3.258581 \times 10^{+00}$	$2.449801 \times 10^{+00}$
SSR	$2.786 \times 10^{-05}$	$2.495 \times 10^{-05}$	$1.067 \times 10^{-05}$	$5.596 \times 10^{-05}$

### $Q_B$ values

$e_\beta(r)$  values calculated with the transfer function method are presented in Table 4. Three columns represent the values of  $e_\beta(r)$  from monoenergetic electrons (conversion and Auger electrons), continuous beta<sup>-</sup>/beta<sup>+</sup> spectra, and progeny of the radionuclide of interest.

Looking at the six reference radionuclides, there are some differences between the IAEA and the source method values. First of all,  $e_\beta(r)$  calculated for <sup>7</sup>Be by the source method and the transfer function method gives different results: 0 with the FLUKA source and  $5.5 \times 10^{-19}$  Sv Bq<sup>-1</sup> h<sup>-1</sup> with the method based on transfer functions. In fact, <sup>7</sup>Be has two internal conversion electrons at around 477 keV with an emission probability of  $1 \times 10^{-10}$  per disintegration in the ICRP nuclear data. In FLUKA v. 2011.2c.6, the nuclear data for <sup>7</sup>Be does not contain any electron emission above 350 keV, which is the energy threshold to reach the skin scoring volume. However, the calculation done with the source method and giving a null value is not illogical because a dose of  $5.5 \times 10^{-19}$  Sv Bq<sup>-1</sup> h<sup>-1</sup>, calculated in this paper, is negligible.

Calculating  $e_\beta(r)$  and  $h_{skin}(r)$  with a transfer function as it is done in this paper is more accurate than with radionuclide source simulations. In this way, effects of electrons or positrons emitted with low probability are not underestimated. When a source of electrons at a specific energy is used to compute the associated dose in a scoring volume, more events are simulated at this specific energy, leading to a better convergence of dose at this energy.

Results for all radionuclides are satisfactory, except for <sup>60</sup>Co, <sup>152</sup>Tb, <sup>156</sup>Tb, <sup>166</sup>Tm, <sup>166</sup>Yb, and <sup>213</sup>Bi (ratios FLUKA source method—transfer function between 1.2 and 2.4),

which cannot be explained by the statistical uncertainty. Two main reasons explain these differences:

- The effect as explained for <sup>7</sup>Be is valid for these radionuclides also, as they emit electrons with low probability in

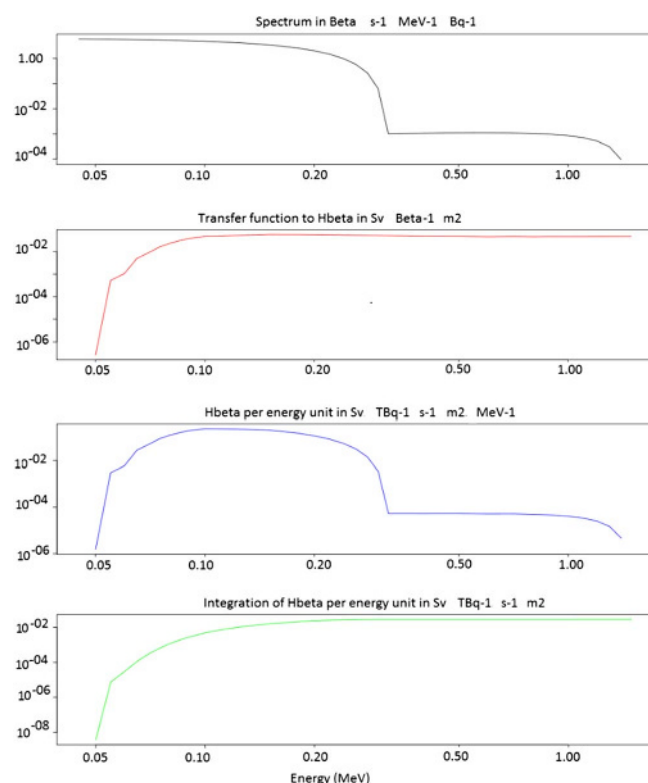


**Fig. 9.** Steps leading to the calculation of  $h_{skin}(r)$ .

**Table 4.** Beta skin dose equivalent  $e_\beta(\gamma)$ , shielded and compared to values from the literature. Values in  $\text{Sv h}^{-1}$  per 1 Bq.

Radionuclide	Progeny to take into account	Decay mode <sup>a</sup>	Half-life	Calculated		Progeny (cont. + mono.)		This paper's method		IAEA (IAEA 2012)		FLUKA source method		GRS (Buttner 2014)	
				shield	A.U.	Sv Bq <sup>-1</sup> h <sup>-1</sup>	Sv Bq <sup>-1</sup> h <sup>-1</sup>	Sv Bq <sup>-1</sup> h <sup>-1</sup>	Sv Bq <sup>-1</sup> h <sup>-1</sup>	Sv Bq <sup>-1</sup> h <sup>-1</sup>	Sv Bq <sup>-1</sup> h <sup>-1</sup>	Sv Bq <sup>-1</sup> h <sup>-1</sup>	Sv Bq <sup>-1</sup> h <sup>-1</sup>	Sv Bq <sup>-1</sup> h <sup>-1</sup>	
<sup>7</sup> Be		EC	53.22 d	3.0	1.6 × 10 <sup>-18</sup>	0.0		5.5 × 10 <sup>-19</sup>	1.0 × 10 <sup>-15</sup>	0.00		4.1 × 10 <sup>-21</sup>			
<sup>22</sup> Na		ECB+	2.6019 y	3.6	7.5 × 10 <sup>-17</sup>	1.0 × 10 <sup>-12</sup>		2.8 × 10 <sup>-13</sup>	2.6 × 10 <sup>-13</sup>	2.9 × 10 <sup>-13</sup>		3.2 × 10 <sup>-13</sup>			
<sup>47</sup> Ca		B-	4.536 d	3.2	1.1 × 10 <sup>-15</sup>	4.9 × 10 <sup>-12</sup>	5.5 × 10 <sup>-13</sup>	1.6 × 10 <sup>-12</sup>	2.7 × 10 <sup>-14</sup>	1.8 × 10 <sup>-12</sup>		1.4 × 10 <sup>-12</sup>			
<sup>58</sup> Co		ECB+	70.86 d	6.8	4.9 × 10 <sup>-15</sup>	4.7 × 10 <sup>-14</sup>		7.6 × 10 <sup>-15</sup>	1.3 × 10 <sup>-15</sup>	7.0 × 10 <sup>-15</sup>		2.0 × 10 <sup>-15</sup>			
<sup>60</sup> Co		B-	5.2713 y	5.0	3.2 × 10 <sup>-15</sup>	1.3 × 10 <sup>-14</sup>		3.3 × 10 <sup>-15</sup>	1.4 × 10 <sup>-15</sup>	2.7 × 10 <sup>-15</sup>		1.8 × 10 <sup>-15</sup>			
<sup>137</sup> Cs	<sup>137m</sup> Ba	B-	30.1671 y	8.3	0.0	1.1 × 10 <sup>-12</sup>	2.0 × 10 <sup>-12</sup>	7.5 × 10 <sup>-13</sup>	1.2 × 10 <sup>-13</sup>	7.2 × 10 <sup>-13</sup>		1.6 × 10 <sup>-13</sup>			
<sup>61</sup> Cu		ECB+	3.3333 h	7.7	1.8 × 10 <sup>-15</sup>	6.7 × 10 <sup>-12</sup>		8.6 × 10 <sup>-13</sup>	—	8.7 × 10 <sup>-13</sup>		—			
<sup>71</sup> As		ECB+	2.72 d	24.9	2.1 × 10 <sup>-15</sup>	2.1 × 10 <sup>-12</sup>		8.3 × 10 <sup>-14</sup>	8.3 × 10 <sup>-14</sup>	—		8.4 × 10 <sup>-14</sup>			
<sup>140</sup> Nd	<sup>140</sup> Pr	EC	3.37 d	3.0	0.0	0.0		6.1 × 10 <sup>-12</sup>	2.3 × 10 <sup>-12</sup>	—		2.3 × 10 <sup>-12</sup>			
<sup>140</sup> Pr		ECB+	3.39 m	2.6	1.0 × 10 <sup>-14</sup>	6.1 × 10 <sup>-12</sup>		2.3 × 10 <sup>-12</sup>	—	—		2.3 × 10 <sup>-12</sup>			
<sup>140</sup> Tb		ECB+A	4.12 h	2.5	9.7 × 10 <sup>-14</sup>	8.9 × 10 <sup>-13</sup>		3.9 × 10 <sup>-13</sup>	—	3.8 × 10 <sup>-13</sup>		2.2 × 10 <sup>-14</sup>			
<sup>152</sup> Tb		ECB+	17.5 h	2.1	3.9 × 10 <sup>-13</sup>	2.3 × 10 <sup>-12</sup>		1.3 × 10 <sup>-12</sup>	—	9.8 × 10 <sup>-13</sup>		1.7 × 10 <sup>-13</sup>			
<sup>155</sup> Tb		EC	5.32 d	3.0	2.2 × 10 <sup>-15</sup>	0.0		7.5 × 10 <sup>-16</sup>	—	—		9.1 × 10 <sup>-18</sup>			
<sup>156</sup> Tb		EC	5.17 d	3.0	9.1 × 10 <sup>-14</sup>	0.0		3.0 × 10 <sup>-14</sup>	—	2.3 × 10 <sup>-14</sup>		2.2 × 10 <sup>-15</sup>			
<sup>161</sup> Tb		B-	6.89 d	102.1	1.7 × 10 <sup>-16</sup>	4.0 × 10 <sup>-13</sup>		3.9 × 10 <sup>-15</sup>	—	4.0 × 10 <sup>-15</sup>		3.5 × 10 <sup>-15</sup>			
<sup>166</sup> Tm		ECB+	7.7 h	3.3	1.2 × 10 <sup>-13</sup>	1.7 × 10 <sup>-13</sup>		8.5 × 10 <sup>-14</sup>	—	2.0 × 10 <sup>-13</sup>		—			
<sup>166</sup> Yb		EC	2.362 d	3.0	0.0	0.0		8.5 × 10 <sup>-14</sup>	—	2.0 × 10 <sup>-13</sup>		4.2 × 10 <sup>-15</sup>			
<sup>209</sup> Tl		B-	2.161 m	3.3	3.0 × 10 <sup>-13</sup>	1.1 × 10 <sup>-11</sup>		3.4 × 10 <sup>-12</sup>	—	3.4 × 10 <sup>-12</sup>		—			
<sup>213</sup> Po/ <sup>209</sup> Tl		ECB+	45.59 m	5.51	1.4 × 10 <sup>-13</sup>	8.4 × 10 <sup>-12</sup>	3.0 × 10 <sup>-17</sup> / 1.1 × 10 <sup>-11</sup>	1.63 × 10 <sup>-12</sup>	—	2.0 × 10 <sup>-12</sup>		1.3 × 10 <sup>-12</sup>			

<sup>a</sup>A.U.: arbitrary units; EC: electron capture; ECB+: electron capture and positron emission; B-: electron emission; ECB+A: electron capture, positron emission, and alpha emission.

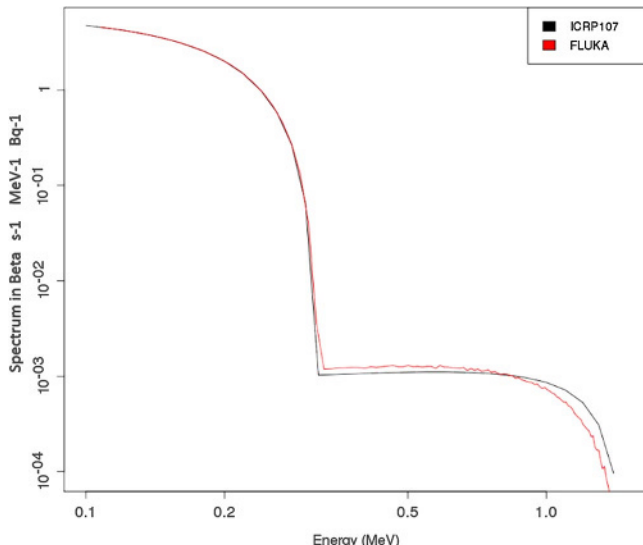


**Fig. 10.** Differences between FLUKA spectrum and ICRP Publication 107 spectrum for  $^{60}\text{Co}$  in beta  $\text{Bq}^{-1} \text{s}^{-1} \text{MeV}^{-1}$ .

the range of importance of the transfer function as shown in Fig. 4; and

- A comparison of the decay data from FLUKA and ICRP Publication 107 (ICRP 2008) has been done for the  $^{60}\text{Co}$  spectrum as can be seen in Fig. 10. The spectrum of the  $^{60}\text{Co}$  decay has been extracted from FLUKA with a FLUKA USRBDX score and compared to the spectrum from ICRP Publication 107, which is used with the transfer function. In the range of important energies, from 0.35 to 2 MeV, the beta spectrum differs. Using the FLUKA spectrum in the transfer function leads to a value of  $2.7 \times 10^{-15} \text{ Sv Bq}^{-1} \text{ h}^{-1}$  for  $e_\beta(r)$ , instead of the  $3.3 \times 10^{-15} \text{ Sv Bq}^{-1} \text{ h}^{-1}$  calculated with the ICRP Publication 107 spectrum, in which monoenergetic electrons were added. So using the FLUKA spectrum with the transfer functions provided the same values as the FLUKA source method.

The difference between the dose calculated by the source method and the transfer function method is fully explained by the differences in nuclear data.

### $Q_D$ values

$h_{\text{skin}}(r)$  values calculated with the transfer function method are presented in Table 5. Three columns represent the values of  $h_{\text{skin}}(r)$  coming from monoenergetic electrons (conversion and Auger electrons), continuous beta<sup>-</sup> or beta<sup>+</sup> spectra, and progeny of the radionuclide of interest.

Looking at the six reference radionuclides compared with IAEA values, significant differences are observed only for  $^7\text{Be}$ . IAEA limits the  $Q$  values to a low

threshold of 1,000 TBq, leading to a minimal value of  $2.8 \times 10^{-5} \text{ Sv s}^{-1} \text{ TBq}^{-1} \text{ m}^2$  for  $Q_D$ . The calculation of  $h_{\text{skin}}(r)$  is easier than the calculation of  $e_\beta(r)$  as there is no attenuation in air to take into account before scoring the dose in skin, explaining why  $h_{\text{skin}}(r)$  results are more comparable to IAEA values than  $e_\beta(r)$  values. For every other radionuclide in Table 5, the comparison between the source method and the transfer function calculation gives comparable results except for  $^{166}\text{Tm}$  and  $^{166}\text{Yb}$ , which are linked by their decay chain.

The explanation of the differences earlier are still valid for  $h_{\text{skin}}(r)$ . The simulation with the FLUKA source method with  $^{166}\text{Tm}$  as the source gives a value of  $4.8 \times 10^{-2} \text{ Sv s}^{-1} \text{ TBq}^{-1} \text{ m}^2$ . The use of the FLUKA spectrum for  $^{166}\text{Tm}$  with the transfer function method gives an  $h_{\text{skin}}(r)$  of  $4.3 \times 10^{-2} \text{ Sv s}^{-1} \text{ TBq}^{-1} \text{ m}^2$ . The value calculated with the ICRP Publication 107 spectrum from this work is  $1.24 \times 10^{-2} \text{ Sv s}^{-1} \text{ TBq}^{-1} \text{ m}^2$ . This shows that differences between the source method and transfer function method come from the nuclear data. Nevertheless, the transfer function method remains more precise for the reasons already given above. Concerning all the other radionuclides, coherence with the literature and with radionuclide source calculations are proven. Calculations with VARSKIN 6.1 have been done using a punctual source geometry to compare with values of this paper (Hamby et al. 2017). The choice of a punctual source geometry in VARSKIN 6.1 has been chosen to be conform to the FLUKA method, as results are normalized to the surface of the source. Comparisons with Global Research for Safety (GRS) codes (Cologne, Germany) and VARSKIN 6.1 show similarities.

## CONCLUSION

This work demonstrates the possibility of calculating  $Q$  values linked to beta emitters with FLUKA. The actual work presents a method that is efficient and precise, and that does not require additional Monte Carlo simulations to produce  $Q$  values for all radionuclides. The goal of this paper is to make data available for all radionuclides which could be of interest for the transport of activated equipment or radionuclides. It also increases the feasibility of calculating beta dose rates with transfer functions. With respect to previously calculated  $Q$  values from IAEA, this work allows for the calculation of all  $Q_B$  and  $Q_D$  values which are not detailed in the literature. Good agreement has been shown for  $Q_B$  and  $Q_D$  coefficients.

Calculations of  $e_{pt}$ ,  $e_\beta$ ,  $e_{inh}$ , and  $h_{\text{skin}}$  have been performed for 1,252 radionuclides and are available in an Excel spreadsheet (Microsoft Corp., Redmond, Washington, US) as supplemental digital content (SDC, <http://links.lww.com/HP/A149>).

**Table 5.** Beta skin dose equivalent  $h_{s,kin}(r)$ , compared to values from the literature. Values in  $\text{Sv}^{-1} \text{per } 1 \text{ TBq m}^{-2}$ .

Radionuclide	Progeny to take into account	Decay mode <sup>a</sup>	Progeny (cont + mono)			IAEA value (IAEA 2012)	FLUKA source method (Butter 2014)	GRS value (Hamby et al. 2017)	VARSKIN 6.1 (Hamby et al. 2017)	Bourgeois value (Bourgeois et al. 2017)
			Half-life	Monoengetic	Continuous					
<sup>7</sup> Be		EC	53.22 d	$3.7 \times 10^{-09}$	0.0	$3.7 \times 10^{-09}$	$2.8 \times 10^{-05}$	0.0	$4.1 \times 10^{-09}$	$3.4 \times 10^{-09}$
<sup>22</sup> Na		ECB+	2.6019 y	$3.2 \times 10^{-07}$	$4.3 \times 10^{-02}$	$4.3 \times 10^{-02}$	$4.2 \times 10^{-02}$	$4.3 \times 10^{-02}$	$3.9 \times 10^{-02}$	$4.0 \times 10^{-02}$
<sup>47</sup> Ca		B-	4.536 d	$3.4 \times 10^{-06}$	$4.5 \times 10^{-02}$	$4.0 \times 10^{-02}$	$8.5 \times 10^{-02}$	$8.4 \times 10^{-02}$	$8.8 \times 10^{-02}$	$7.9 \times 10^{-02}$
<sup>58</sup> Co		ECB+	70.86 d	$1.5 \times 10^{-05}$	$7.3 \times 10^{-03}$	$7.3 \times 10^{-03}$	$7.4 \times 10^{-03}$	$7.5 \times 10^{-03}$	$1.2 \times 10^{-03}$	$6.9 \times 10^{-03}$
<sup>60</sup> Co		B-	5.2713 y	$1.4 \times 10^{-05}$	$2.9 \times 10^{-02}$	$2.9 \times 10^{-02}$	$2.9 \times 10^{-02}$	$2.9 \times 10^{-02}$	$3.0 \times 10^{-02}$	$2.7 \times 10^{-02}$
<sup>137</sup> Cs	<sup>137m</sup> Ba	B-	30.1671 y	$1.8 \times 10^{-08}$	$4.0 \times 10^{-02}$	$4.8 \times 10^{-03}$	$4.5 \times 10^{-02}$	$4.4 \times 10^{-02}$	$4.6 \times 10^{-02}$	$4.1 \times 10^{-02}$
<sup>61</sup> Cu		ECB+	3.333 h	$3.1 \times 10^{-05}$	$3.0 \times 10^{-02}$	$3.0 \times 10^{-02}$	$—$	$3.0 \times 10^{-02}$	$2.0 \times 10^{-02}$	$2.8 \times 10^{-02}$
<sup>71</sup> As		ECB+	2.72 d	$4.5 \times 10^{-03}$	$1.4 \times 10^{-02}$	$1.9 \times 10^{-02}$	$—$	$1.8 \times 10^{-02}$	$8.8 \times 10^{-03}$	$1.7 \times 10^{-02}$
<sup>140</sup> Pr		EC	3.37 d	0.0	$2.4 \times 10^{-02}$	$2.4 \times 10^{-02}$	$—$	$2.4 \times 10^{-02}$	$1.5 \times 10^{-02}$	$2.4 \times 10^{-02}$
<sup>140</sup> Pr		ECB+	3.39 m	$5.6 \times 10^{-05}$	$2.4 \times 10^{-02}$	$2.4 \times 10^{-02}$	$—$	$2.4 \times 10^{-02}$	$—$	$2.4 \times 10^{-02}$
<sup>149</sup> Tb		ECB+A	4.12 h	$9.3 \times 10^{-03}$	$3.4 \times 10^{-03}$	$1.3 \times 10^{-02}$	$—$	$1.2 \times 10^{-02}$	$9.7 \times 10^{-03}$	$1.2 \times 10^{-02}$
<sup>152</sup> Tb		ECB+	17.5 h	$3.1 \times 10^{-03}$	$9.3 \times 10^{-03}$	$1.2 \times 10^{-02}$	$—$	$1.0 \times 10^{-02}$	$5.4 \times 10^{-03}$	$1.2 \times 10^{-02}$
<sup>155</sup> Tb		EC	5.32 d	$6.8 \times 10^{-03}$	0.0	$6.8 \times 10^{-03}$	$—$	$6.5 \times 10^{-03}$	$6.8 \times 10^{-03}$	$4.9 \times 10^{-03}$
<sup>156</sup> Tb		EC	5.17 d	$1.9 \times 10^{-02}$	0.0	$1.9 \times 10^{-02}$	$—$	$1.8 \times 10^{-02}$	$1.9 \times 10^{-02}$	$1.4 \times 10^{-02}$
<sup>161</sup> Tb		B-	6.89 d	$1.4 \times 10^{-04}$	$3.8 \times 10^{-02}$	$3.8 \times 10^{-02}$	$—$	$3.8 \times 10^{-02}$	$3.9 \times 10^{-02}$	$3.6 \times 10^{-02}$
<sup>166</sup> Tm		ECB+	7.7 h	$1.2 \times 10^{-02}$	$6.2 \times 10^{-04}$	$1.2 \times 10^{-02}$	$—$	$4.8 \times 10^{-02}$	$—$	$9.6 \times 10^{-03}$
<sup>166</sup> Tb		EC	2.362 d	$2.1 \times 10^{-03}$	0.0	$1.2 \times 10^{-02}$	$—$	$4.7 \times 10^{-02}$	$1.1 \times 10^{-02}$	$1.1 \times 10^{-02}$
<sup>209</sup> Tl		B-	2.161 m	$4.5 \times 10^{-03}$	$4.7 \times 10^{-02}$	$5.1 \times 10^{-02}$	$—$	$5.0 \times 10^{-02}$	$—$	$4.8 \times 10^{-02}$
<sup>213</sup> Bi		<sup>213</sup> Po <sup>209</sup> Tl	45.59 m	$2.7 \times 10^{-03}$	$4.5 \times 10^{-02}$	$8.1 \times 10^{-08}$	$4.8 \times 10^{-02}$	$8.7 \times 10^{-02}$	$5.0 \times 10^{-01}$	$4.5 \times 10^{-01}$
						$1.2 \times 10^{-02}$				$3.6 \times 10^{-02}$

<sup>a</sup>EC: electron capture; ECB+: electron capture and positron emission; B-: electron emission; ECB+A: electron capture, positron emission, and alpha emission.

## REFERENCES

Battistoni G, Boehlen T, Cerutti F, Wai Chin P, Salvatore Esposito L, Fasso A, Ferrari A, Lechner A, Empl A, Mairani A, Mereghetti A, Ortega PG, Ranft J, Roesler S, R. Sala P, Vlachoudis V, Smirnov G. Overview of the FLUKA code. *Annals Nucl Energy* 82:10–18; 2015.

Behrens R. Compilation of conversion coefficients for the dose to the lens of the eye. *Radiat Protect Dosim* 174:348–370; 2017. DOI 10.1093/rpd/ncw194.

Benassai S, Bologna L. Re-evaluation of  $Q_A$  and  $Q_B$  values on the basis of complete spectra for gamma, x, and beta emissions. Rome: National Agency for Environmental Protection; ANPA-DIR/NOR-RT-2; 1994.

Bourgeois L, Néard S, Comte N. Calculation of skin dose due to beta contamination using the new quantity of the ICRP 116: the local skin dose. *Radiat Protect Dosim* 176:365–379; 2017. DOI 10.1093/rpd/ncx019.

Buttner U. Surveying on the safety of transport of radioactive material. Part 1.1. Calculation of activity limits model; final report on work package 4. Cologne: Global Research for Safety; GRS-343; 2014 (in German).

Eckerman KF, Ryman JC. External exposure to radionuclides in air, water and soil. Washington, DC: US Environmental Protection Agency; Federal Guidance Report 12, EPA-402-R-93-081; 1993.

Ferrari A, Sala P, Fasso A, Ranft J. FLUKA: a multi-particle transport code. Stanford, CA: SLAC; CERN 2005-10, INFN/TC\_05/11, SLAC-R-773; 2005.

Hamby DM, Mangini CD, Shaffer V, Bush-Goddard SP. VARSkin 6: a computer code for skin contamination dosimetry. Washington, DC: US Nuclear Regulatory Commission; NUREG/CR-6913/Rev. 3; 2017.

International Atomic Energy Agency. Advisory material for the IAEA regulations for the safe transport of radioactive material. Vienna: IAEA; Specific safety guide SSG-26; 2012.

International Commission on Radiological Protection. Compendium of dose coefficients based on ICRP Publication 60. Oxford: ICRP; Publication 119; 2012.

International Commission on Radiological Protection. Nuclear decay data for dosimetric calculations. Oxford: ICRP; Publication 107; 2008.

International Commission on Radiological Protection. Conversion coefficients for radiological protection quantities for external radiation exposures. Oxford: ICRP; Publication 116; 2010.

International Commission on Radiation Units and Measurements. Quantities and units in radiation protection dosimetry. Bethesda, MD: ICRU; Report 51; 1993.

Japan Atomic Energy Research Institute. Dose coefficients for radionuclides produced in high energy proton accelerator facilities: coefficients for radionuclides not listed in ICRP Publications. Tokai-mura, Japan: JAERI; JAERI-data/code 2002-013; 2002.

Nowotny R. XMuDat: photon attenuation data on PC; version 1.0.1 [online]. 1998. Available at <https://www-nds.iaea.org/publications/iaea-nds/iaea-nds-0195.htm>. Accessed 1 January 2018.

Petoussi N, Zankl M, Fehrenbacher G, Drexler G. Dose distribution in the ICRU sphere for monoenergetic photons and electrons and for ca. 800 radionuclides. Institut für Strahlenschutz. GSF-Bericht 7/93; 1993.

Veinot K, Hertel N. Personal dose equivalent conversion coefficients for electrons to 1 GeV. *Radiat Protect Dosim* 149: 347–352; 2010. DOI 10.1093/rpd/ncq380.

